Journal of Materials Chemistry A

Rapid thermal annealing of $CH_3NH_3PbI_3$ perovskite thin films by intense pulsed light with aid of diiodomethane additive

Journal:	*Journal of Materials Chemistry A*
Manuscript ID	TA-COM-02-2018-001237.R2
Article Type:	Communication
Date Submitted by the Author:	27-Apr-2018
Complete List of Authors:	Ankireddy, Krishnamraju; University of Louisville, Conn Center for Renewable Energy Research Ghahremani, Amir; University of Louisville, Conn Center for Renewable Energy Research Martin, Blake; University of Louisville, Conn Center for Renewable Energy Research Gupta, Gautam; University of Louisville, Conn Center for Renewable Energy Research Druffel, Thad; University of Louisville, Conn Center for Renewable Energy Research

Journal of Materials Chemistry A

COMMUNICATION

Rapid thermal annealing of $CH_3NH_3PbI_3$ perovskite thin films by intense pulsed light with aid of diiodomethane additive

Received 00th January 20xx,
Accepted 00th January 20xx

DOI: 10.1039/x0xx00000x

www.rsc.org/

Krishnamraju Ankireddy,[a] Amir H. Ghahremani,[a,b] Blake Martin,[a,b] Gautam Gupta [a,b] and Thad Druffel,*[a]

The organic metal halide perovskite material is capable of high throughput manufacturing via traditional deposition processes used in roll-to-roll, yet thermal annealing post deposition may require long ovens. We report rapid annealed perovskite thin films using intense pulsed light (IPL) to initiate a radiative thermal response that is enabled by an alkyl halide additive that collectively improves the performance of a device processed in an ambient environment from a baseline of 10% to 16.5% efficiency. Previous reports on $CH_3NH_3PbI_3$ perovskite films using IPL processing achieved functional devices in milli-second time scales and are promising for high throughput manufacturing processes under ambient conditions. In this study, we found that the addition of diiodomethane (CH_2I_2) as an additive to the methylammonium iodide (MAI) / lead iodide (PbI_2) precursor ink chemistry and subsequent IPL thermal annealing are inter-dependent. The concentration of CH_2I_2 and IPL processing parameters have a direct effect on the surface morphology of the films and performance within a perovskite solar cell (PSC). The CH_2I_2 dissociates under exposure to ultraviolet (UV) radiation from the IPL source liberating iodine ions in the film, influencing the perovskite formation and reducing the defect states. We anticipate that these results can be utilized to further develop different ink formulations using alkyl halides for the IPL technique to improve the performance of perovskite solar cells processed in ambient conditions.

The perovskite solar cell (PSC) has made significant improvements in photovoltaic performance with confirmed efficiencies of over 20%.[1] The design of the device also allows for embedding other materials within the active layers thereby extending absorption into the near infrared wavelengths.[2] Enhancements to the durability through substitution of the organic cation[3] and demonstrations of large area production[4, 5] are moving the technology towards greater commercial viability. These accomplishments are predominately achieved using solution phase techniques, where precursors are dispersed in solvent at relatively low concentrations resulting in a formulation with low viscosity. These formulations can then be deposited directly onto a substrate using evaporative techniques such as spin, spray and blade coating. The thickness, roughness and coverage of the perovskite film Is extremely important in producing high performance PSC.[6] The nucleation of the perovskite during the single step deposition is understood to occur as the solvent evaporates shifting the precursor materials into a supersaturation state within the solvent which leads to precipitation. He et al utilized a meniscus-assisted solution printing technique that promotes the crystallization at the edge of the meniscus.[7] Anti-solvents are often deposited during the latter stages of the spin coating to accomplish the nucleation.[8-11] Engineering of the precursor solvents using co-solvents and additives have been shown to improve the light harvesting and stability as well as reducing the hysteresis of the PSC.[12] Subsequent grain growth during an annealing step is then completed through thermal techniques.[13] However, the boundary between the nucleation and grain growth is not necessarily distinct and often includes solvent/perovskite intermediaries.[14] This both complicates and yields opportunities towards the formation of high quality perovskite grains for application in the PSC. This interplay between precursor chemistries and solvents during deposition has been demonstrated for several ABX_3 perovskite chemistries, where the A cation is from methylammonium, formamidinium, cesium, the B metal is Pb or Sn and the X halide is chlorine, bromine and iodine or mixtures thereof. The simplest and most widely studied perovskite material is $CH_3NH_3PbI_3$, where the precursor chemistries include PbI_2 and MAI.

The thermal annealing techniques are normally realized through direct conduction (hot-plates) or convection (ovens) and generally require dwell time scale of tens of minutes.[15, 16] The main concern with the thermal processes is that the $CH_3NH_3PbI_3$ is limited to low temperatures (150°C), before the methylammonium cation sublimates leading to degradation. A

[a] University of Louisville, Conn Center for Renewable Energy Research, Louisville, KY 40292 USA. *Email: thad.druffel@louisville.edu
[b] University of Louisville, Department of Chemical Engineering, Louisville, KY 40292 USA

Electronic Supplementary Information (ESI) available: [details of any supplementary information available should be included here]. See DOI: 10.1039/x0xx00000x

cation substitution including formamidinium and cesium not only improves the durability of the materials, but also increases the thermal stability of the perovskite thin films.[17] It has been shown that the formamidinium/methylammonium cation mixture can be processed to temperatures of up to 400°C, which can significantly reduce the solvent evaporation and annealing times.[18] Among different annealing techniques, vacuum flash annealing process is one type of approach in which the atmospheric pressure is reduced to well below the vapor pressure of the solvents improving the film morphology through removal of DMF but still requires a thermal annealing step.[19] In another approach, radiative heating is utilized to induce a localized heating in the perovskite film through the absorption of light energy reducing the thermal annealing time. This radiative heating has been used in the semiconductor industry via a rapid thermal annealing (RTA) technique wherein light, often infrared (IR), absorbed by crystalline silicon results in a significant increase in temperature within the wafer. The broad absorption of light exhibited by the perovskite material makes it an ideal choice for RTA processes. The RTA technique has been demonstrated for the $CH_3NH_3PbI_3$ system in which process and formulation optimization allowed for annealing to occur in just a few minutes.[20] Similar to RTA, another rapid annealing technique called Intense pulsed light (IPL) heats a thin film using light energy, but the wavelengths span from the UV to the visible (vis) into the near infrared (NIR) and the duration of the pulse is on the order of a millisecond. This method has been applied to the $CH_3NH_3PbI_3$ perovskite deposited using a two-step method (PbI_2 spin coating followed by MAI dip coat) initiating temperatures of 750°C for less than 1 millisecond.[21] However, the two-step deposition previously described along with the requirement of an inert atmosphere is non-ideal for roll-to-roll manufacturing and hence, a single step perovskite deposition process under a low humidity condition was opted for this work.

This study expands the deposition of the $CH_3NH_3PbI_3$ material in low humidity ambient air and subsequently processed in an IPL apparatus without humidity controls. The IPL technique has the potential to anneal the perovskite material at speeds of several square meters per second in ambient conditions. The IPL equipment features a halogen lamp that can deliver up to 36 J/cm^2 over a 60 cm^2 area during the 1-2 ms flash.[22] The process is enabled by the use of an additive, CH_2I_2, a light sensitive alkyl halide, that enhances the overall performance of the solar cell through improved surface coverage and charge carrier dynamics. The role of alkyl halides in the crystal formation, solvent and solute interaction, and influence on the film surface morphology has been explored for the films processed using thermal annealing processes but not explored with photonic annealing techniques.[23, 24] The interaction of the IPL and CH_2I_2 are probed using scanning electron microscopy, X-ray diffraction, electroimpedance spectroscopy and concludes with an optimization of the IPL conditions and CH_2I_2 concentrations.

To establish the process for depositing $CH_3NH_3PbI_3$ films, a spin coater was retrofitted with a dry air inlet to reduce the humidity in the spin coater chamber to well below 10%. In this study, the formulation includes DMF and DMSO, which is well known to form an adduct of DMSO-perovskite during the evaporation of the DMF. This is often precipitated using an anti-solvent such as chlorobenzene, which we have also employed in this work. However, after the spin coating step, the perovskite layer turned-out to be a transparent film which was not ideal for IPL annealing in which white light must be absorbed to initiate thermal annealing. Therefore, films were placed on the hot plate at 75°C for 2 min under ambient conditions to initiate the nucleation process. The films turned to brownish in color from transparent and subsequently, the films were appropriate for the IPL process. The IPL process was accomplished using a Sinteron 2000 by Xenon Corporation, where the films were exposed to five flashes each having a duration of two milliseconds with an energy density of 25 J/cm^2 per flash (unless otherwise stated). The IPL processing of these neat perovskite cells yielded a device with an efficiency of 10% (fig. 1A). The addition of the CH_2I_2 to the formulation and processing using the IPL significantly improved the overall performance of the device to 16.5% (Fig. 1A). The short circuit

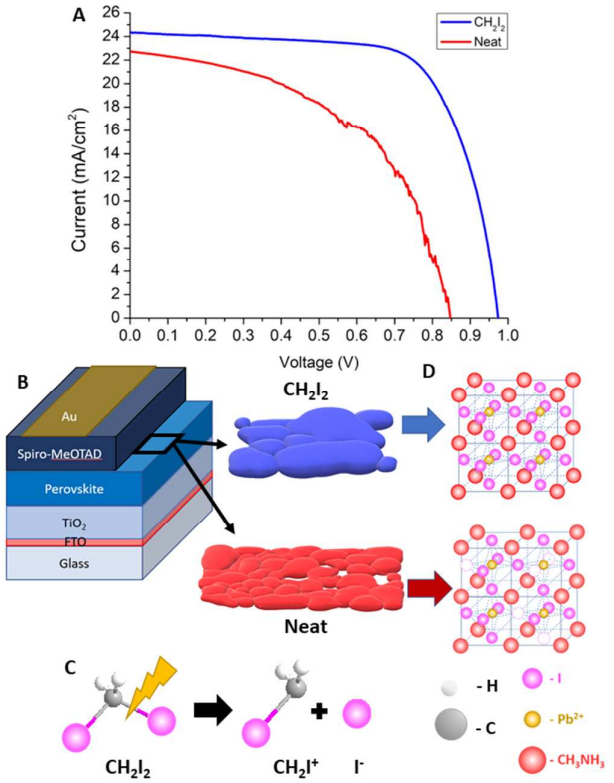

Fig. 1 Schematic explanation of the improved results with the CH_2I_2 additive in the CH3NH3PbI3 perovskite solar cell leading to A) improved photovoltaic performance. B) Structure of the PSC used in this study where the perovskite fits between a TiO2 hole blocking layer and a Spiro-MeOTAD hole transport layer. The direct effect of the CH_2I_2 additive improves the sur-face coverage of the solar cell. C) Cleavage of the CH_2I_2 additive under exposure to UV releasing an iodide ion that can D) fill iodide vacancies improving the ionic conductivity of the film.

current (J_{sc}), open circuit voltage (V_{oc}) and fill factor (FF) each saw a large improvement with the addition of the CH_2I_2. The champion cell exhibited a power conversion efficiency (PCE) of 16.5%, FF of 69.6, V_{oc} of 0.97 V and J_{sc} of 24.3 mA/cm^2 and the average performance from 10 CH_2I_2-perovskite cells are shown in Table 1. Current densities over 24 mA/cm^2 have been previously reported where the improvement was attributed to an additional iodine source in the precursor solution or modification of electron transport layers.[25-29]

Table 1. Average performance of neat and CH_2I_2 perovskite solar cells (neat – 5 samples, CH_2I_2 – 10 samples)

	J_{sc}	V_{oc}	FF	PCE
Neat	21.7	0.84	44.4	8.0
	± 2.9	± 0.03	± 6.2	± 1.4
CH_2I_2	23.7	0.99	65.1	15.3
	± 0.7	± 0.03	± 3.0	± 1.4

Based on the experimental results, we propose that CH_2I_2 plays multiple roles in initial deposition of the films as well as post-processing of the films with IPL technique. First, CH_2I_2 improves the solvent-precursor interaction which promotes quality and coverage of the $CH_3NH_3PbI_3$ films as observed elsewhere with alkyl halide additives (Fig. 1B). Second, the IPL cleaves the CH_2I_2 producing disassociated iodide ions (Fig. 1C) that participate in the perovskite crystal formation (Fig. 1D). The increased cell performance can be attributed to oriented pore-free films influenced by the interaction of the IPL and CH_2I_2 causing lower charge recombination at grain boundaries and decreased shunt resistance pathways (Fig. 2).

The low performance of the neat cells is attributed to the poor morphology as evidenced by the numerous pin-holes (Fig. 2A). The addition of the CH_2I_2 influenced the crystal growth by controlling the grain growth and allowing the solute-solvent interaction to obtain a pin hole free perovskite film formation (Fig. 2B). Several additives have been proposed to improve the morphology of the perovskite thin films including polymers, organic precursors, alkylhalides, where these are reported to improve the surface coverage of the perovskite during the deposition.[30] The use of alkyl halides was specifically explored by Chueh et al and showed that these additives influenced the film morphology and thus improved performance in all cases.[23] The absorbance of the two films are very similar across the visible wavelengths and both samples were brownish in color (Fig. 2G). However, it was observed that the neat films were hazy producing a diffuse reflectance from the surface (Fig 2H). The CH_2I_2 films were clear and exhibited a specular reflectance (Fig 2I). This is indicative that the CH_2I_2 films were more homogenous and smooth.

The role of the CH_2I_2 additive on the film crystallinity was investigated by conducting XRD analysis on neat and CH_2I_2 perovskite films. The XRD analysis reveals that despite the high temperatures experienced by the film during IPL processing, pure perovskite films were produced with no lead iodide formation as the major lead iodide peak at 12.6° was absent in the films (Fig. 2 C&D). In addition, diffraction peaks at 14.06°, 19.9°, 23.4°, 24.4°, 28.4°, 31.8°, 34.9°, 40.5°, 43° and 50.5° were assigned to (110), (112), (211), (202), (220), (310), (312), (224), (314) and (404) crystal planes, respectively, indicate the perovskite was formed in tetragonal crystal structure.[31] The

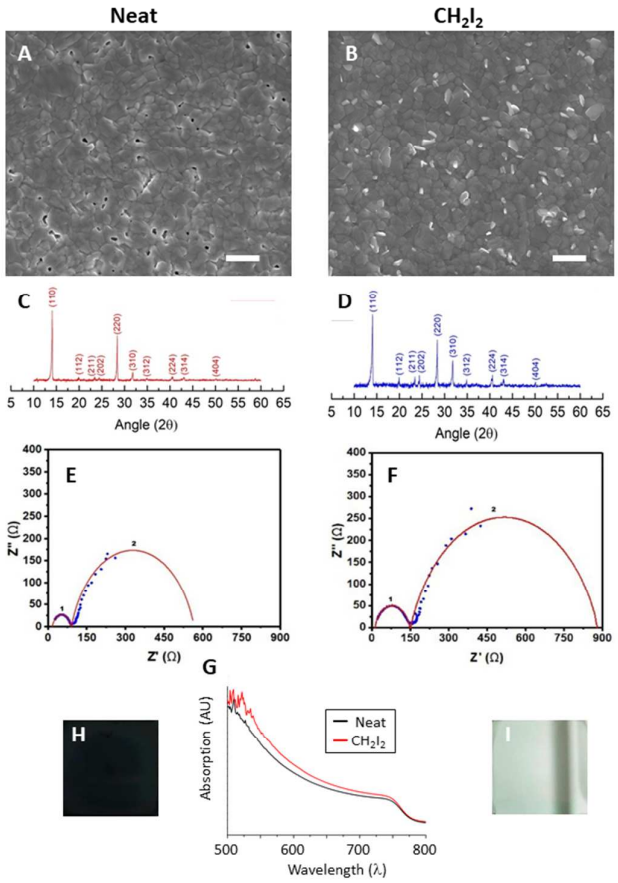

Fig. 2 Side by side comparison of results neat (left) and CH_2I_2 additive (right) perovskite films processed using IPL. A,B) Scanning electron microscope image showing a pinhole free surface with the addition of CH_2I_2.(Scale bar is 1 micron) C,D) XRD diffraction pattern with no obvious degradation to the films. E,F) EIS scans demonstrating a higher series recombination resistances in the CH_2I_2 film G) UV-vis absorption of the films and H,I) photographs of the perovskite films.

intense peaks at (110) and (220) planes imply the formation of highly uniform and oriented perovskite structures.

The perovskite solar cell performance is improved upon addition of CH_2I_2 with IPL treatment as shown in Fig. 1. To understand this phenomenon, neat and CH_2I_2 perovskite solar cells were compared using electroimpedance spectroscopy (EIS) (Fig. 2 E&F).[32] Neat and CH_2I_2 cells were held at a potential near their respective open-circuit voltages (V_{oc}) and the frequency was swept from ~1E106 Hz to ~0.01 Hz. At high frequencies, we expect impedance signals indicative of series resistance within the cell. Signal 1 in Fig. 2E is smaller than signal 1 in Fig. 2f suggesting that there is less series resistance in the neat perovskite cell than the CH_2I_2 perovskite cell. This result would suggest that the neat perovskite cell would perform better than the CH_2I_2 perovskite cell. However, the

change in resistance is negligible and the dominant effect is due to the change in the recombination resistance. The low frequency region of the EIS plot is indicative of recombination resistance within the perovskite material. Recombination within a solar cell is detrimental to performance; therefore, an increase in recombination resistance is expected to improve the performance of the cell. Signal 2 in Fig. 2E is smaller than signal 2 in Fig. 2f suggesting that the neat perovskite cell has lower recombination resistance than the CH_2I_2 perovskite cell. The CH_2I_2 additive in combination with IPL treatment improved the recombination resistance implying that these modifications are the source of the performance increase.

It is widely known that CH_2I_2 can be cleaved with UV energy,[33] and the IPL equipment can be tuned to energies from the UV through to the NIR and hence the primary reason the CH_2I_2 alkyl halide was chosen for this study. The C-I bond in CH_2I_2 possesses 50 kcal/mol which can be cleaved by light and/or thermal energy. In this case, IPL provides optimum conditions to cleave the C-I bonds as it provides UV as well as thermal energy. To confirm the CH_2I_2 dissociation with IPL light energy, a CH_2I_2-perovskite cell was prepared by subjecting the perovskite film to the IPL light energy but blocking the UV portion of the spectrum. The cells exhibited large hysteresis with very low fill factor which indirectly indicates the incomplete bond cleavage or dissociation of iodine ions in the perovskite film (Supporting information Fig. S1). Chueh et al confirmed the participation of iodide from alkyl halide additives in the perovskite formation.[23] The XRD patterns and the absorption band-edge in UV spectra of the perovskite films processed from MACl + $PbCl_2$ + 1,4-Diiodobutane (DIB) formula are almost identical to that of conventional $CH_3NH_3PbI_{3x}Cl_x$ processed from 3MAI + $PbCl_2$. Since 1,4-DIB is the only source for iodide, this result indicates that the C–I bond in 1,4-DIB was cleaved and the resulting iodide participated in the crystallization process of perovskite. The formation of deep-level defects, such as interstitial and antisite defects, which are responsible for nonradiative recombination centers in perovskite layers, depends on I-poor or I-rich conditions.[34-36] Buin et al found that the presence in solution of simple ions (Pb^{2+} and I^-) combined with that of lead-iodide complex anions such as PbI^{3-}, PbI_4^{2-}, and PbI_5^{3-} produces a motif similar to the PbI^0 neutral antisite defect which corresponds to bridging between three iodine anions in-plane and interplane in the perovskite lattice. The motif is produced indirectly, by violating local stoichiometry. It was predicted that the perovskite grown under I-rich conditions will show a high density of deep traps that will curtail the diffusion length.[35]

Recent studies have shown that moderate excessive iodine inclusion in the precursor solution yielded less defects in the perovskite films and thus increased efficiencies[25, 37] Yang et al introduced additional iodide ions into the dripping solution, which facilitated the fabrication of perovskite films with a certified efficiency of 22.1%. The maximum efficiency was attained when the dripping solution contained 3 mmol of I^-_3 and further increase in the iodine concentration in the dripping solution resulted in decreasing trend in the efficiencies. Jalebi et al added potassium iodide to introduce excess iodide into the perovskite precursor solutions for compensating any halide vacancies. It was expected that the excess halides fill the halide vacancies and thus passivate the nonradiative recombination whereas potassium immobilize the excess halide and thus inhibiting halide migration.

In order to find the optimal CH_2I_2 concentration and IPL process parameters for influencing halide vacancies, three different concentration of CH_2I_2 in the solution was investigated (figure 3A). Among three different concentrations of CH_2I_2 (0.125, 0.25, and 0.375 ml per 1ml DMF and 0.125 ml DMSO solvent mixture), 0.25 ml CH_2I_2 added (0.25 CH_2I_2) perovskite cells showed the highest efficiency. Further increase of CH_2I_2 in the solution resulted in decrease in the efficiency. It might be the case where optimized CH_2I_2 (0.25 ml) concentration is introducing moderate excessive iodine ions to replenish halide vacancies due to some of CH_3NH_3I sublimation and inherent vacancies formed during film formation. Higher than optimized concentration of CH_2I_2 might be creating excessive Iodine rich conditions and causing high density of deep traps. Interestingly the J-V graphs show that the differentiation in performance is evident from the FF, whereas the J_{sc} and V_{oc} remain relatively stable (Figure 3). The EIS and J-V characteristics confirms the higher recombination resistance and better efficiencies from CH_2I_2 added perovskite films compared to neat perovskite films. Furthermore, the improvement in the hysteresis with the addition of the CH_2I_2 can also be attributed to the better management of iodide ion

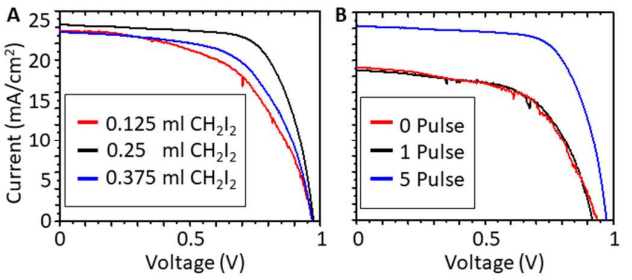

Fig. 3 I-V results of A) varying the concentration of the CH_2I_2 additive and B) varying the total number of pulses.

vacancies in the films.

The role of IPL process on the film formation was also investigated by changing the number of pulses while holding the energy density constant. Three different conditions were tested: no-IPL, 1 IPL pulse and 5 IPL pulses. The performance of the PSC samples again shows that there is an obvious change with IPL processing and in this case the V_{oc} and J_{sc} are impacted (figure 3B). It is evident that a single pulse was not sufficient to increase the performance of the device as there is very little change. However, 5 pulses delivered sufficient energy to have a major impact on the performance of the PSC device. Increasing the number of pulse to 10 (not shown here) produces a non-working device. Further investigation is required to fully understand the effect of concentration of CH_2I_2 and IPL conditions on the perovskite formation.

These results imply that unlike traditional thermal sintering, the IPL process might influence the crystal growth in a different way. The IPL process introduces very high

temperatures up to 700 ^{o}C to the film, depending on the input energy density given to the IPL source, and dissipate the thermal energy in millisecond time scale. During this spike in the temperature of the film, some of the MAI might sublimate from the film and could cause iodide poor conditions more than needed for ideal iodine poor conditions to lower the defect density. This sublimation of MAI during perovskite film formation from the laser sintering method has been observed.[38] The addition of CH_2I_2 might be replenishing iodide ions with the aid of IPL process in C-I bond cleavage and thus reducing overall defect densities in the perovskite film. The EIS results from CH_2I_2-perovskite films confirms the lower defect densities compared to neat films. However, the synergy between CH_2I_2 and IPL process in forming perovskite films is a complex phenomenon and further investigation is undertaken to fully understand the perovskite formation.

We have successfully fabricated high efficiency perovskite solar cells by adding light sensitive CH_2I_2 as an additive to MAI and PbI_2 ink chemistry and annealing the films rapidly using IPL technique under ambient conditions. The additive added perovskite films exhibited pin hole free surface coverage after subjecting to IPL process whereas the neat perovskite films exhibited incomplete coverage of the film. In addition, the concentration of the CH_2I_2 in the ink chemistry and different IPL processing conditions directly influenced the efficiency of the perovskite cells. The impedance spectroscopy analysis on the CH_2I_2 and neat perovskite cells qualitatively revealed the lower recombination rate for the CH_2I_2 perovskite cells. As a result, perovskite solar cells with efficiencies up to 16.5 % were produced with IPL processing. Clearly, the devices built without the IPL process were functional and others have shown high efficiency with longer soak times at higher temperatures; however, the IPL process enables a much faster conclusion to the annealing step. The process can also be done in ambient conditions without humidity control.

It should be pointed out, that the V_{oc} of the cells produced in this study was less than 1 Volt, which is low for the $CH_3NH_3PbI_3$ PSC. This is attributed to the annealing occurring in ambient conditions at uncontrolled humidity. The synergy between IPL processing and CH_2I_2 additive is not fully understood and further investigation of the CH_2I_2 interaction with IPL process, influence of different methylammonium halides on the IPL processing, film morphology, and defect states is required. Future work will also include the triple cation perovskites, which are more tolerant to humidity. This study also included a short conductive thermal process to initiate the nucleation of the perovskite material such that it could absorb the photonic energy. Unfortunately, this is inherent to the spin coating method; however, other scalable techniques such as spray could eliminate this need.

Acknowledgments

The authors acknowledge the Conn Center for Renewable Energy Research at the University of Louisville for their financial support and research facilities.

References

1. M. A. Green, Y. Hishikawa, W. Warta, E. D. Dunlop, D. H. Levi, J. Hohl-Ebinger and A. W. H. Ho-Baillie, *Progress in Photovoltaics: Research and Applications*, 2017, **25**, 668-676.
2. M. He, X. Pang, X. Liu, B. Jiang, Y. He, H. Snaith and Z. Lin, *Angew Chem Int Ed Engl*, 2016, **55**, 4280-4284.
3. L. Jin-Wook, K. Deok-Hwan, K. Hui-Seon, S. Seung-Woo, C. S. M. and P. Nam-Gyu, *Advanced Energy Materials*, 2015, **5**, 150310.
4. S. Razza, F. Di Giacomo, F. Matteocci, L. Cinà, A. L. Palma, S. Casaluci, P. Cameron, A. D'Epifanio, S. Licoccia, A. Reale, T. M. Brown and A. Di Carlo, *J. Power Sources*, 2015, **277**, 286-291.
5. W. Chen, Y. Wu, Y. Yue, J. Liu, W. Zhang, X. Yang, H. Chen, E. Bi, I. Ashraful, M. Gratzel and L. Han, *Science*, 2015, **350**, 944-948.
6. M. He, D. Zheng, M. Wang, C. Lin and Z. Lin, *J. Mater. Chem. A*, 2014, **2**, 5994-6003.
7. M. He, B. Li, X. Cui, B. Jiang, Y. He, Y. Chen, D. O'Neil, P. Szymanski, M. A. Ei-Sayed, J. Huang and Z. Lin, *Nat Commun*, 2017, **8**, 16045.
8. Y. Zhou, M. Yang, W. Wu, A. L. Vasiliev, K. Zhu and N. P. Padture, *J. Mater. Chem. A*, 2015, **3**, 8178-8184.
9. N. G. Park, *Nano Converg.*, 2016, **3**, 15.
10. S. Paek, P. Schouwink, E. N. Athanasopoulou, K. T. Cho, G. Grancini, Y. Lee, Y. Zhang, F. Stellacci, M. K. Nazeeruddin and P. Gao, *Chem. Mater.*, 2017, **29**, 3490-3498.
11. K.-M. Lee, C.-J. Lin, B.-Y. Liou, S.-M. Yu, C.-C. Hsu, V. Suryanarayanan and M.-C. Wu, *Sol. Energy Mater Sol. Cells*, 2017, **172**, 368-375.
12. M. Ye, C. He, J. Iocozzia, X. Liu, X. Cui, X. Meng, M. Rager, X. Hong, X. Liu and Z. Lin, *Journal of Physics D: Applied Physics*, 2017, **50**.
13. Z. Song, S. C. Watthage, A. B. Phillips, B. L. Tompkins, R. J. Ellingson and M. J. Heben, *Chem. Mater.*, 2015, **27**, 4612-4619.
14. H. Zhou, Q. Chen, G. Li, S. Luo, T. B. Song, H. S. Duan, Z. Hong, J. You, Y. Liu and Y. Yang, *Science*, 2014, **345**, 542-546.
15. A. Dualeh, N. Tétreault, T. Moehl, P. Gao, M. K. Nazeeruddin and M. Grätzel, *Adv. Funct. Mater.*, 2014, **24**, 3250-3258.
16. G. E. Eperon, V. M. Burlakov, P. Docampo, A. Goriely and H. J. Snaith, *Advanced Functional Materials*, 2014, **24**, 151-157.
17. M. Saliba, T. Matsui, J. Y. Seo, K. Domanski, J. P. Correa-Baena, M. K. Nazeeruddin, S. M. Zakeeruddin, W. Tress, A. Abate, A. Hagfeldt and M. Gratzel, *Energy Environ. Sci.*, 2016, **9**, 1989-1997.
18. M. Kim, G. H. Kim, K. S. Oh, Y. Jo, H. Yoon, K. H. Kim, H. Lee, J. Y. Kim and D. S. Kim, *ACS Nano*, 2017, **11**, 6057-6064.
19. X. Li, D. Bi, C. Yi, J. D. Decoppet, J. Luo, S. M. Zakeeruddin, A. Hagfeldt and M. Gratzel, *Science*, 2016, **353**, 58-62.
20. B. Dou, V. L. Pool, M. F. Toney and M. F. A. M. van Hest, *Chem. Mater.*, 2017, **29**, 5931-5941.
21. B. W. Lavery, S. Kumari, H. Konermann, G. L. Draper, J. Spurgeon and T. Druffel, *ACS Appl. Mater. Interfaces*, 2016, **8**, 8419-8426.
22. T. Druffel, R. Dharmadasa, B. W. Lavery and K. Ankireddy, *Sol. Energy Mater Sol. Cells*, 2018, **174**, 359-369.

23. C.-C. Chueh, C.-Y. Liao, F. Zuo, S. T. Williams, P.-W. Liang and A. K. Y. Jen, *Journal of Materials Chemistry A*, 2015, **3**, 9058-9062.
24. Z. Liang, S. Zhang, X. Xu, N. Wang, J. Wang, X. Wang, Z. Bi, G. Xu, N. Yuan and J. Ding, *RSC Adv.*, 2015, **5**, 60562-60569.
25. W. S. Yang, B. W. Park, E. H. Jung, N. J. Jeon, Y. C. Kim, D. U. Lee, S. S. Shin, J. Seo, E. K. Kim, J. H. Noh and S. I. Seok, *Science*, 2017, **356**, 1376-1379.
26. A. Huang, L. Lei, J. Zhu, Y. Yu, Y. Liu, S. Yang, S. Bao, X. Cao and P. Jin, *ACS Appl Mater Interfaces*, 2017, **9**, 2016-2022.
27. Q. Jiang, L. Zhang, H. Wang, X. Yang, J. Meng, H. Liu, Z. Yin, J. Wu, X. Zhang and J. You, *Nature Energy*, 2016, **2**.
28. X. Huang, Z. Zhao, L. Cao, Y. Chen, E. Zhu, Z. Lin, M. Li, A. Yan, A. Zettl, Y. M. Wang, X. Duan, T. Mueller and Y. Huang, *Science*, 2015, **348**, 1230-1234.
29. T. Singh, S. Öz, A. Sasinska, R. Frohnhoven, S. Mathur and T. Miyasaka, *Advanced Functional Materials*, 2018, **28**.
30. P. W. Liang, C. Y. Liao, C. C. Chueh, F. Zuo, S. T. Williams, X. K. Xin, J. Lin and A. K. Jen, *Adv. Mater.*, 2014, **26**, 3748-3754.
31. Z. Bi, Z. Liang, X. Xu, Z. Chai, H. Jin, D. Xu, J. Li, M. Li and G. Xu, *Sol. Energy Mater Sol. Cells*, 2017, **162**, 13-20.
32. G. Garcia-Belmonte, P. P. Boix, J. Bisquert, M. Sessolo and H. J. Bolink, *Solar Energy Materials and Solar Cells*, 2010, **94**, 366-375.
33. A. N. Tarnovsky, J.-L. Alvarez, A. P. Yartsev, V. Sundstrom and E. Akesson, *Chem. Phys. Lett.*, 1999, **312**, 121-130.
34. A. Buin, R. Comin, J. Xu, A. H. Ip and E. H. Sargent, *Chem. Mater.*, 2015, **27**, 4405-4412.
35. A. Buin, P. Pietsch, J. Xu, O. Voznyy, A. H. Ip, R. Comin and E. H. Sargent, *Nano Lett.*, 2014, **14**, 6281-6286.
36. R. J. Stewart, C. Grieco, A. V. Larsen, G. S. Doucette and J. B. Asbury, *J. Phys. Chem. C*, 2016, **120**, 12392-12402.
37. M. Abdi-Jalebi, Z. Andaji-Garmaroudi, S. Cacovich, C. Stavrakas, B. Philippe, J. M. Richter, M. Alsari, E. P. Booker, E. M. Hutter, A. J. Pearson, S. Lilliu, T. J. Savenije, H. Rensmo, G. Divitini, C. Ducati, R. H. Friend and S. D. Stranks, *Nature*, 2018, **555**, 497-501.
38. F. Li, W. Zhu, C. Bao, T. Yu, Y. Wang, X. Zhou and Z. Zou, *Chem Comm.*, 2016, **52**, 5394-5397.

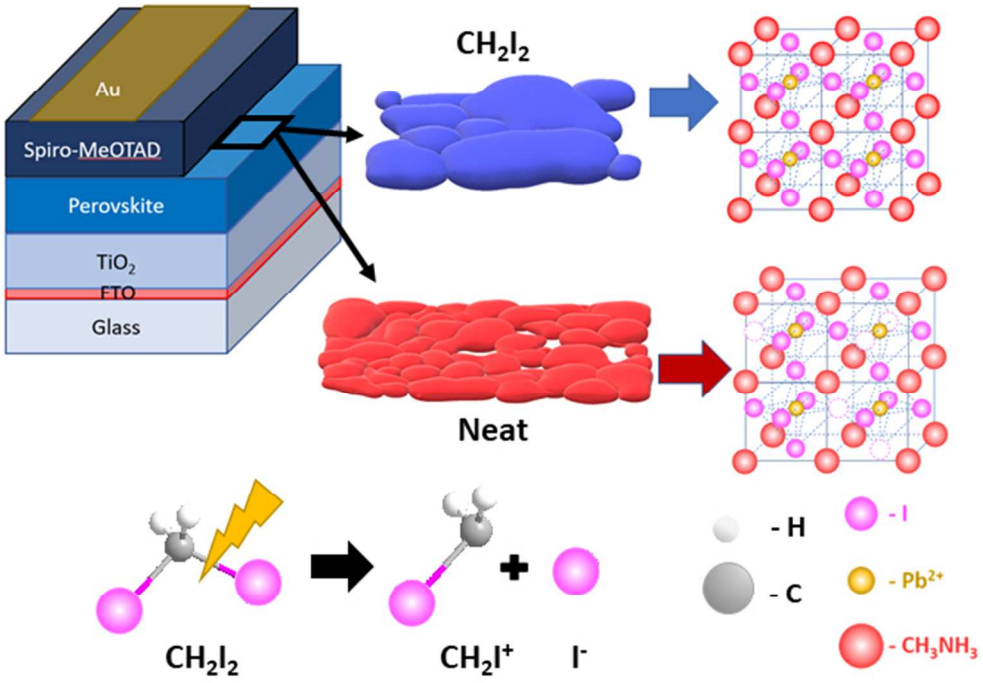

179x126mm (96 x 96 DPI)